A STUDY ON THERMAL BARRIER COATINGS INCLUDING THERMAL EXPANSION MISMATCH AND BOND COAT OXIDATION*

George C. Chang and Woraphat Phucharoen
Cleveland State University

Robert A. Miller
National Aeronautics and Space Administration
Lewis Research Center

1. INTRODUCTION

The present investigation deals with a plasma-sprayed thermal barrier coating (TBC) intended for high temperature applications to advanced gas turbine blades. Typically, this type of coating system consists of a zirconia-yttria ceramic layer with a nickel-chromium-aluminum bond coat on a superalloy substrate. The problem on hand is a complex one due to the fact that bond coat oxidation and thermal mismatch occur in the TBC, as reported in reference 1. Cracking in the TBC has also been experimentally illustrated in the same reference.

The purpose of this investigation is to help achieve a clearer understanding of the mechanical behavior of the TBC. The near-term objective is to study the stress states in a model thermal barrier coating as it cools down in air.

In this investigation, the powerful finite element method has been utilized to model a coated cylindrical specimen. Four successively refined finite element models have been developed. Some results obtained using the first two models have been reported in references 2, 3 and 4.

The present paper discusses progress in the current year. The major accomplishment is the successful development of an elastic TBC finite element model known as TBCG with interface geometry between the ceramic layer and the bond coat. An equally important milestone is the near-completion of the new elastic-plastic TBC finite element model called TBCGEP which yielded initial results. Representative results are presented in figures 11 through 22.

2. EXPERIMENTAL FINDINGS OF FRACTURING OF COATINGS

A number of researchers have reported their TBC work since the late 1970's. Most papers and reports dealt with testing of coated specimen ranging from cylindrical coupons to full-size turbine blades. Significant progress has been made, however, the central question of coating failure mechanism(s) has yet to be conclusively ascertained.

Of particular interest to the present investigation is the experimental work on TBC reported in reference 1. In that work, coated superalloy specimens were

* Research conducted under NASA-CSU Cooperative Research Agreement No. NCC-3-27

tested. The uncoated specimen which is illustrated in figure 1, had a radius of 0.65 cm. and a length of 7.60 cm. The specimens were plasma-sprayed in air with the zirconia-yttria (ZrO_2-8wt.% Y_2O_3) on a nickel-chromium-aluminum-zirconium bond coat. Coated specimens were next exposed to the combustion gases of a burner rig for varying periods of time before cooling took place. Most specimens went through many thermal cycles.

In reference 1, it was found that the coatings of all specimens tested in the air at temperatures high enough permitting bond coat oxidation eventually failed in spalling. The spalling which was visible had been examined by scanning electron microscopy (SEM) to be preceded by ceramic coating delamination. The TBC specimens invariably failed within the ceramic layer just above the bond coat on cooling in air from high temperatures. The same photomicrographs also showed the rough interface between the ceramic layer and the bond coat that contained oxides. More oxides were found in the region adjacent to the interface than the region away from the interface. Some interfaces were approximately sinusoidal with peak-to-peak and peak-to-valley dimensions up to 100 micrometers (μm).

These tests illustrated some TBC failure modes, and have led to the present analytical modeling effort.

3. FINITE ELEMENT MODELING OF A CYLINDRICAL THERMAL BARRIER COATING

To determine the quantitative nature of the stress (and strain) states associated with a TBC specimen, a general-purpose finite element program has been employed to model a cylindrical test specimen which is similar to the ones reported in reference 1. The modeling concept is illustrated in figure 1.

The test specimen is sufficiently long, as compared to its radius, that the problem can be approximated by a two-dimensional generalized plane-strain case. This approximation implies, as in the classical theory of elasticity, uniform strain in the axial (or z-) direction. The chief advantage of this approximation is to help keep the amount of computation to a manageable level on a super computer.

As shown in figure 1, a sinusoidal interface between the ceramic layer and the bond coat is introduced with a period of approximately 50 μm (0.0020 in.) and an amplitude of approximately 15 μm (0.0006 in.). This interface is much smoother than the one (50 μm) used for the results reported earlier in reference 4.

The three materials comprising the substrate, the bond coat, and the ceramic are assumed to be homogeneous and isotropic and elastic for the TBCG model. The bond material in the latest model, TBCGEP, however, is assumed to be elastic-plastic, following the classical theory of plasticity with von Mises' criterion for yielding or the onset of plastic flow. Strain hardening which has been built into the program, is controlled by the slope of the stress-strain curve. Up to four line segments can be used to specify the stress-strain curve associated with the bond material.

Each material, therefore, possesses its own temperature-dependent parameters, such as Young's modulus (E), Poisson's ratio (ν), and thermal expansion coefficient (α). In addition, the bond material has a plasticity parameter which

controls the yielding process (YP1). Finally, the bond material is capable of simulating oxidation effects in the manner discussed in reference 3 and 4, and elsewhere in this paper.

An overview of the more recent (third) model known as TBCG is given in figures 2 to 6. The model contains 1316 nodal points and 2140 elements, both triangular and quadrilateral. Particular attention has been given to the region in the vicinity of the model of fundamental interest in the discretization process. Most elements in the refined region are sized at several micrometers to insure fine resolution. Details of the refined region are shown in figures 7 to 10, where oxidized elements are shown in bold lines along the sinusoidal interface.

The actual modeling is done with the use of a general purpose computer program known as MARC (ref. 5) which is operational on a super computer (CRAY-I) at NASA Lewis Research Center.

The boundary conditions applied to the model are fully compatible with those normally required in the theory of continuum mechanics. More specifically, only radial displacements are allowed to take place along radial lines, OA and OB, in figures 2 and 3. Line AB is free to displace. Point O which represents the center of the unit slice or the z-axis of the cylindrical specimen, is fixed.

Model TBCGEP is identically the same as TBCG, with the exception of plasticity capability in the bond coat.

To simplify the complex problem on hand, only a uniform temperature field is imposed on the model specimen. The steady-state solution sought here will greatly aid in the interpretation of computational results.

4. STRESS STATES CAUSED BY THERMAL EXPANSION MISMATCH

With the use of the TBCG computer program, a problem simulating a cylindrical TBC specimen experiencing a temperature drop of 100°C from an assumed stress-free state at 700°C has been solved. This problem is referred to as Case B-2 which is identically the same as Case A-2 reported in reference 3 with only one difference. In the present case, a smoother ceramic-bond interface with an amplitude of 15 μm is specified. The corresponding magnitude for Case A-2 is 50 μm.

Material properties used for the present case are given in Table 1. Selected results of Case B-2 are shown in figures 11 through 13. The strains are of reasonable size and distribution, being analogous to the stresses. They are not presented here to keep the length of this paper to a proper limit.

From figure 11, it can be seen that stresses in the x-direction (or radial stresses) in the vicinity of the sine peak (asperity) are rather high and are tensile. Such high tensile stresses could easily initiate cracking at the asperities as the TBC specimen cools down. Note these stresses correspond to a temperature drop of 100°C. An additional temperature drop would produce proportionately increased stresses. Thus, there should be little doubt that micro-cracking could be initiated at the asperities at some point during the cooling process. This is especially convincing when one recalls that the occurrence of such

cracking may contribute to the acoustic emission observed as TBC specimens cool down (ref. 6).

The peak tensile radial stresses in figure 11 are only 55 percent as large as those found in Case A-2. The same is also true of the compressive radial stresses between the two cases. This reduction in stress buildup can be most logically attributed to the changing geometry between the two cases. A smoother interface causes less stress concentrations than a rougher interface.

The stresses in the y-direction (or hoop stresses), as shown in figure 12, are fairly uniform throughout the thickness of the ceramic layer. They are compressive, as expected. These stresses are only slightly smaller in magnitude than corresponding values for Case A-2. The reduction is in the range of about ten percent. The same is true of shearing stresses for both Cases B-2 and A-2. Again, the shearing stress maximizes near the interface where failure is observed in reference 1. At present, reliable data on allowable stresses from this ceramic material is lacking. It is therefore inappropriate to make any conclusive remarks about these two stresses, although the shearing stress is of significant magnitude (± 8 MPa).

5. STRESS STATES ASSOCIATED WITH BOND-COAT OXIDATION

Reference 1 reported that bond coat oxidation was seen to grow with thermal cycles when the test was conducted in the air. The failure of TBC was correlated with this oxidation of the bond coat. The oxide layer appeared to grow thicker with each exposure to the air at high temperature. The net effect is equivalent to inserting an extra oxide layer between the ceramic layer and the remaining unoxidized bond material. The oxide is largely alumina which is a very hard and strong material. As such, the stress state in the ceramic (and the bond) is expected to be severely impacted by the expanding oxide layer.

As a first attempt to model the effects of bond coat oxidation, the single layer of finite elements bordering on the sinusoidal interface have been assigned the properties of alumina. These are given in Table 1.

In this case, oxide growth has been represented by giving these elements an artificially large thermal expansion coefficient given by

$$\alpha_a = G \times \alpha$$

where G is a growth factor, and α is the usual thermal expansion coefficient of the oxide material (7.79×10^{-6}). Proper choice of G was discussed in reference 3.

For the present case, B-10, the growth factor, G, was set equal to -1000. A temperature drop of only 0.1°C was utilized to minimize thermal expansion mismatch stresses. This yielded a very modest expansion of 0.08% in the oxide layer. The resulting stresses due to this oxidation-like process are shown in figures 14 to 16.

The stresses obtained for Case B-10 are, in general, the reverse of those obtained for Case B-2. In figure 14, stresses in the x-direction are compressive near the peak of the asperity and tensile above the valley. Stresses in the

y-direction, as shown in figure 15, are positive near the peak of the asperity while still being negative elsewhere. Shearing stresses in figure 16, are, in general, in the opposite direction (opposite sign).

The magnitude of the above stresses are very large considering that only a very modest expansion of the oxide has been modeled. In particular, the size of tensile radial stresses in the ceramic above the valley is noteworthy. They are in the range of 6 to 10 MPa. Thus, the stress state due to oxidation can be expected to have a profound influence on the coating failure mechanism.

The present case is identically the same as Case A-10 reported in reference 3 with the only exception of interface geometry, the present case involves a smoother interface than Case A-10. As expected, radial stresses in case B-10 are approximately 15 percent lower than those of Case A-10. The overall pattern for radial stresses for Case B-10 is the same as that for Case A-10. The same can be said of patterns of hoop and shearing stresses between these two cases.

6. STRESS STATES RESULTING FROM THERMAL EXPANSION MISMATCH AND PRECRACKING

As radial stresses of large magnitude occur in the ceramic layer at the peak of the asperity accompanied by in-plane compressive stresses, such as shown in figures 11 and 12, cracking in the tangential (or hoop) direction may very well take place. Once cracks occur, the local stress states will be altered. The results of the TBCG calculation for a pre-selected, simulated crack are shown in figures 17 through 19. This problem is labeled Case B-14. The stresses correspond to a temperature drop of 100°C. The radial stresses in figure 17 have been redistributed in the presence of the crack. High tensile radial stresses continue to exist near crack tips, possibly causing additional circumferential cracking. Therefore, crack propagation is entirely expected. However, the magnitudes of such radial tensile stresses are expected to become progressively lower as the crack continues to grow in the circumferential direction. It is also noted that some compressive radial stresses do exist above the valley. Such compression is thought to be able to arrest (or at least slow down) the continued cracking in the absence of other forces (such as those resulting from oxidation) which promote crack growth. This stress phenomenon helps explain the previous observation made in reference 1, that TBC specimens which did not experience oxidation had a long thermal cycle life (e.g. in excess of 10,000 cycles).

Radial stresses at a considerable distance away from the pre-cracking are left almost unchanged from that of Case B-2, as expected. The same is also true with stresses in the y-direction and shearing stresses.

Results of a similar problem, Case A-14, were presented in reference 4. A comparison between the two sets of results indicates that stress patterns in both cases are very much similar, with the present case yielding a reduction of approximately 10 percent in stresses due to the presence of a smoother ceramic-bond interface. This observation is both logical and consistent with two other comparisons made earlier in this paper (in Sections 4 and 5).

7. PRELIMINARY RESULTS OF PLASTICITY IN THE BOND COAT

Initial operational capability of the newest computer program called TBCGEP was achieved in July 1986. This program has been designed to model the cylindrical TBC specimen with an elastic-plastic bond coat. By choice, the ceramic layer and the superalloy substrate remain elastic. Other than this plastic material property, all other features of TBCGEP are identically the same as those of the computer program TBCG.

Results of a preliminary elastic-plastic TBC run known as Case EP-2, are presented in figures 20 through 22. The problem parameters for the case under consideration are given in Table 1. The data used are nearly identical to those of Case B-2. However, a temperature drop of 0.1°C was utilized in this case on a trial basis. (This will also pave the way for successive calculations to accommodate plastic flow/strain hardening.) At the same time, the plasticity yield parameter (YP1) was arbitrarily set at 69 MPa for lack of proper data for the bond coat yielding behavior. (An experimental effort is underway to determine plastic behavior of a related bond coat material. Results from this particular testing are expected to be used for future TBCGEP runs).

The elastic-plastic results presented in figures 20 to 22 are necessarily preliminary in nature. The radial stresses in the bond coat are modest in magnitude. It is premature to draw any specific conclusions from these very limited numerical results of Case EP-2. However, the radial stress pattern in the ceramic, as shown in figure 20, is seen as somewhat similar to that of Case B-2, figure 11. The magnitudes of the elastic-plastic radial stresses in the ceramic are only a small fraction of that of the elastic case. Such low level of stresses could nevertheless be increased, or decreased, by the proper selection of the YP1 value for the bond coat material. As discussed in reference 7, it is generally understood that plasticity leads to the loss of energy in a loaded body, resulting in a somewhat lowered state of stresses than a similar elastic body subjected to the same loads and boundary conditions. In addition, the size of temperature drop will influence the state of stress as well. Thus, these radial stresses in the ceramic are presented here merely as an illustration of the plausible pattern. Considerable effort will be made to quantitatively interpret the meaning of several elastic-plastic runs in the future.

The same can also be said about the states of stresses in the y-direction and of the shearing stresses. Nonetheless, the low state of stress in the y-direction in the bond coat near the peak of asperity is noteworthy. Such a pattern is in clear contrast to that of the stress in the x-direction in the same region.

8. A PRELIMINARY MECHANISM FOR OXIDATION-INDUCED COATING FAILURE

In reference 3, a preliminary mechanism for oxidation-induced coating failure was proposed, as shown in figure 23. The results presented in preceding sections lend additional credibility to that proposed mechanism.

The proposed TBC failure mechanism is largely based on the elastic stress patterns. The actual mechanism would most likely be further complicated by the effects of inelasticity and anisotropy. Nevertheless, it appears that the current computer modeling effort has begun to provide important insights into the thermomechanical behavior of the thermal barrier coatings. Additional

elastic-plastic computer analyses planned for the next eight months will certainly contribute to the evaluation of the validity of the proposed mechanism.

9. CONCLUDING REMARKS

From the preceding discussions in Sections 4 through 6, it is not difficult to suggest that a rough ceramic-bond interface introduces states of higher stresses, as expected. This is a tradeoff the designer will have to deal with.

The capability to generate a reasonably useful set of data pertaining to the cylindrical TBC specimen now exists, along with a limited amount of data (presented here and in references 2, 3 and 4.) These are now available for use by designers or researchers who are interested in TBC failure by either oxidation or fracture caused stress intensities.

With the attainment of initial operational capability of the latest (and fourth) computer program called TBCGEP, several computer runs will be made to calculate stresses and strains in the cylindrical TBC specimen with an elastic-plastic bond coat capable of strain hardening following yielding. Experimental data on the strength and plastic behavior of the bond material, as well as the ceramic, would be of utmost usefulness to this modeling effort. The numerical data so generated by the TBCGEP model should be illustrative of the elastic-plastic behavior of the thermal barrier coating in a comprehensive way hitherto-before considered impossible. Such data could, in turn, guide the experimentalist and the designer in their work on the TBC.

The approach or methodology developed in this investigation is applicable to analyzing any TBC specimens or engine parts protected by related coatings. The latest program, the TBCGEP, can be modified to deal with more complex geometry, where necessary. The only limitation at present time is the computing power. Nevertheless, it is believed that a reasonable modeling effort of a coated turbine blade can now be attempted.

REFERENCES

1. Miller, R. A.; and Lowell, C. E.: Failure Mechanism of Thermal Barrier Coatings Exposed to Elevated Temperatures. Thin Solid Films, 95, 1983, pp. 265 - 273.

2. Chang, G. C.; and Phucharoen, W.: Finite Element Analysis of Thermal Barrier Coatings. NASA - Industry Workshop on Thermal Barrier Coatings, Middleburg Heights, May 1985.

3. Chang, G. C.; Phucharoen, W.; and Miller, R. A.: Thermal Expansion Mismatch and Oxidation in Thermal Barrier Coatings. NASA CP-2405, pp. 405 - 425, 1985.

4. Chang, George C.; Phucharoen, Woraphat; and Miller, Robert A.: Behavior of Thermal Barrier Coatings for Advanced Gas Turbine Blades. Surface and Coatings Technology, 1986 (in-print).

5. Anonymous: MARC Finite Element Program User Manual, Version K-1, MARC Analysis Research Corp., 1983.

6. Berndt, Christopher C.; and Miller, Robert A.: Failure Analysis of Plasma-Sprayed Thermal Barrier Coatings. NASA Technical Memorandum No. 83777, 1984.

7. Chang, George C.: Interaction of Plane Stress Waves With Lined or Unlined Tunnels in Elastic-Perfectly Plastic Media, Ph.D. thesis, University of Illinois, Urbana, Illinois, June 1966.

TABLE 1 MATERIAL AND OTHER PARAMETERS

PARAMETERS	Case B-2	Case B-10	Case B-14	Case EP-2
Young's Modulus (MPa)				
Substrate	$0.1758X10^{6}$	$0.1758X10^{6}$	$0.1758X10^{6}$	$0.1758X10^{6}$
Bond Coat	$0.1379X10^{6}$	$0.1379X10^{6}$	$0.1379X10^{6}$	$0.1379X10^{6}$
Oxide Layer	---	$0.3448X10^{6}$	---	---
Ceramic	$0.0276X10^{6}$	$0.0276X10^{6}$	$0.0276X10^{6}$	$0.0276X10^{6}$
Poisson's Ratio				
Substrate	0.25	0.25	0.25	0.25
Bond Coat	0.27	0.27	0.27	0.27
Oxide Layer	---	0.32	---	---
Ceramic	0.25	0.25	0.25	0.25
Coefficient of Thermal Expansion (/C)				
Substrate	$13.91X10^{-6}$	$13.91X10^{-6}$	$13.91X10^{-6}$	$13.91X10^{-6}$
Bond Coat	$15.16X10^{-6}$	$15.16X10^{-6}$	$15.16X10^{-6}$	$15.16X10^{-6}$
Oxide Layer	---	$-7.79X10^{-3}$	---	---
Ceramic	$10.01X10^{-6}$	$10.01X10^{-6}$	$10.01X10^{-6}$	$10.01X10^{-6}$
Cracks	NO	NO	YES	NO
Temperature Drop	-100°C	-0.1°C	-100°C	-0.1°C

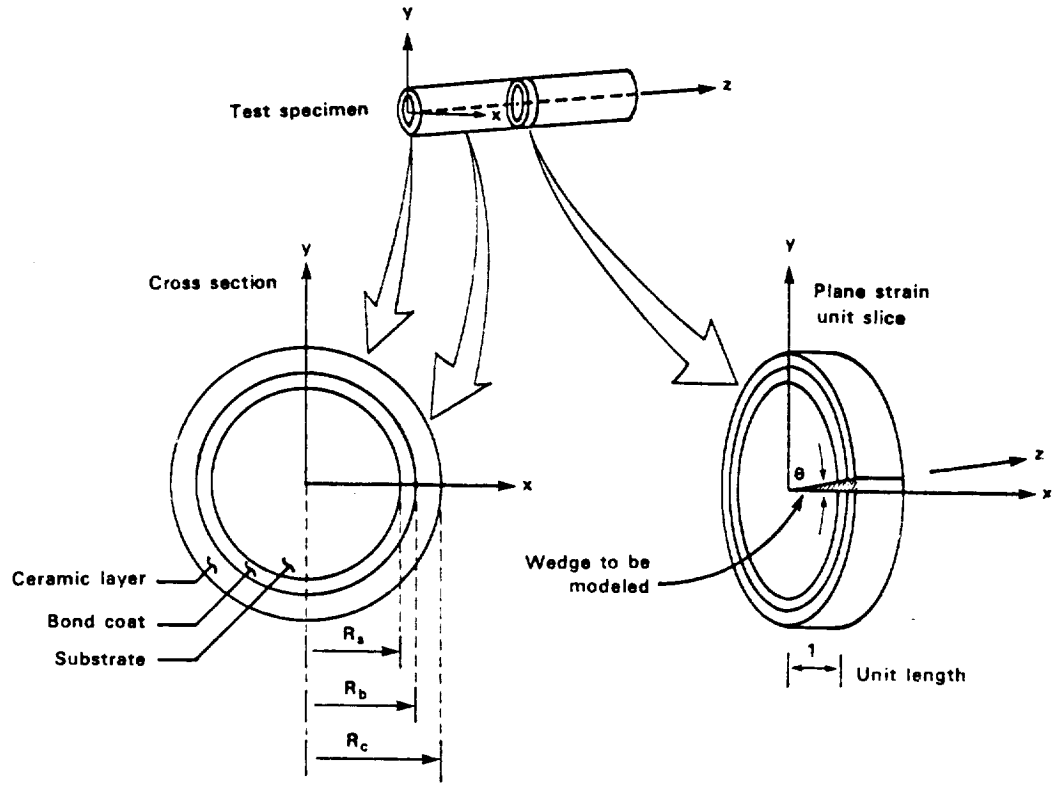

Figure 1. CYLINDRICAL TBC TEST SPECIMEN

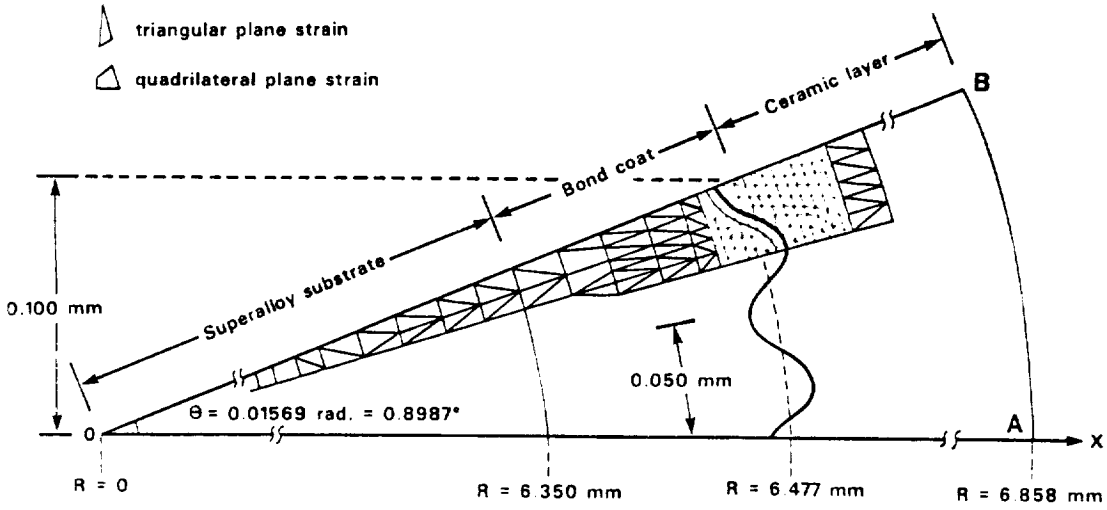

Figure 2. THE TBCG FINITE ELEMENT MODEL

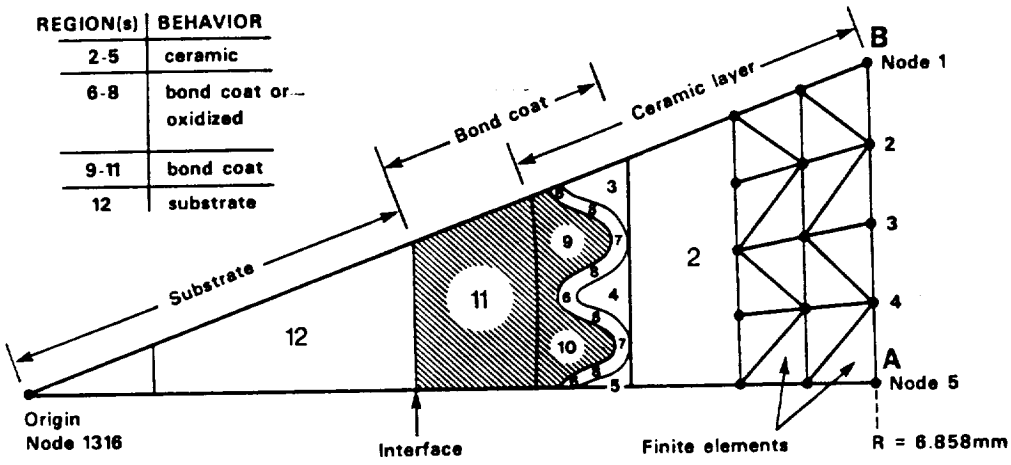

Figure 3. OVERVIEW OF THE ADVANCED TBCG MODEL

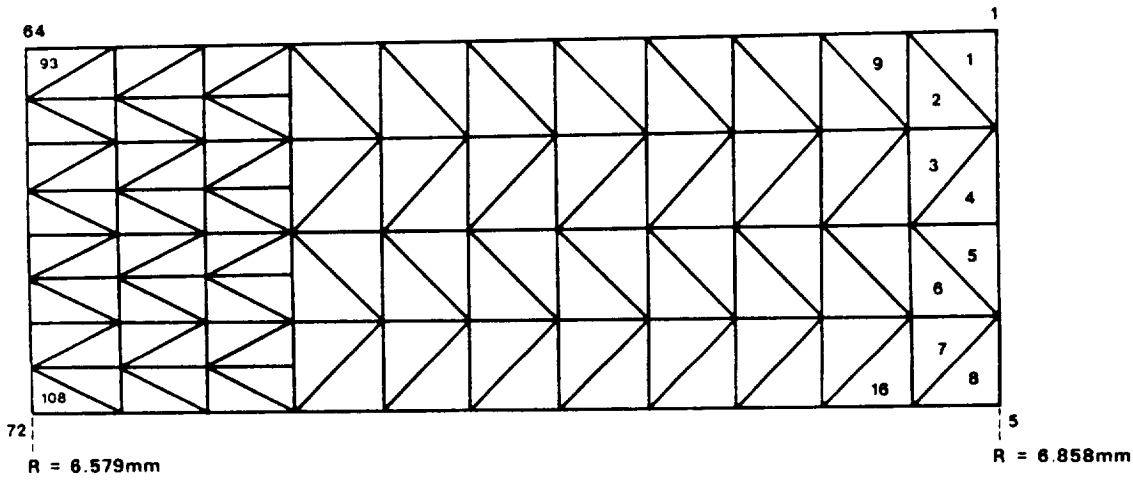

Figure 4. TBCG MODEL (Part 1)

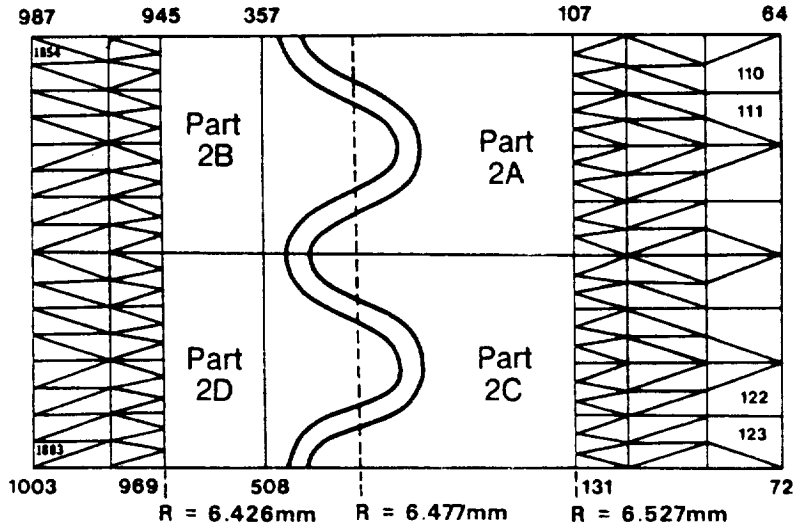

Figure 5. TBCG MODEL (Part 2)

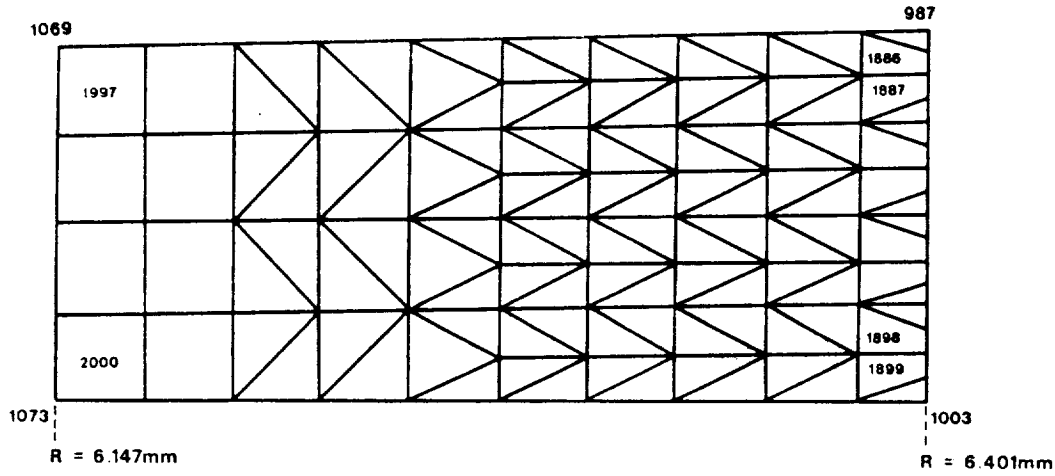

Figure 6. TBCG MODEL (Part 3)

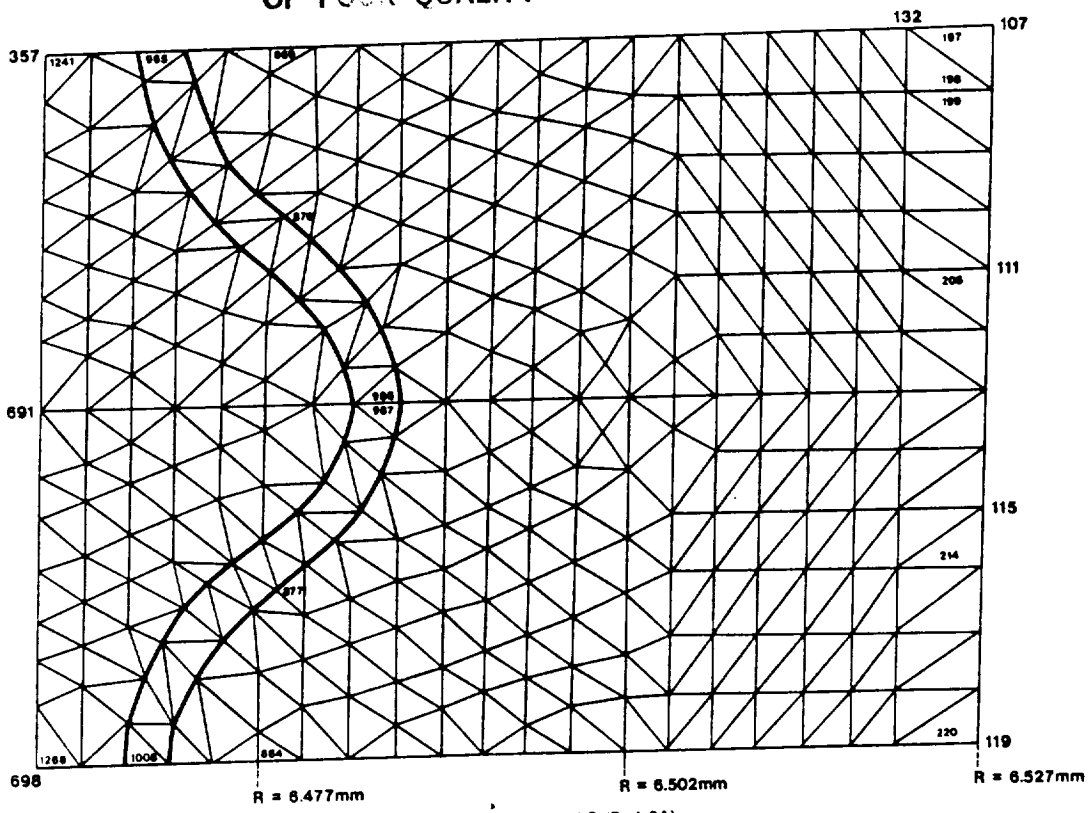

Figure 7. FINITE ELEMENT DETAILS (Part 2A)

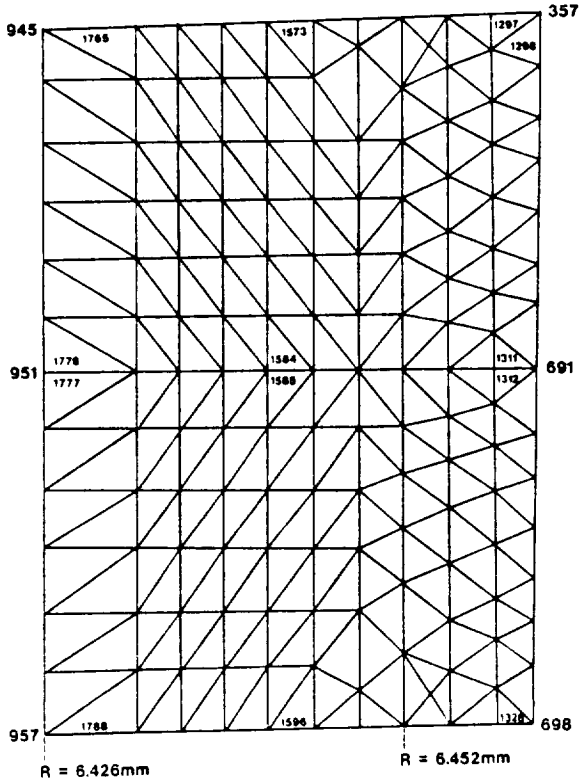

Figure 8. FINITE ELEMENT DETAILS (Part 2B)

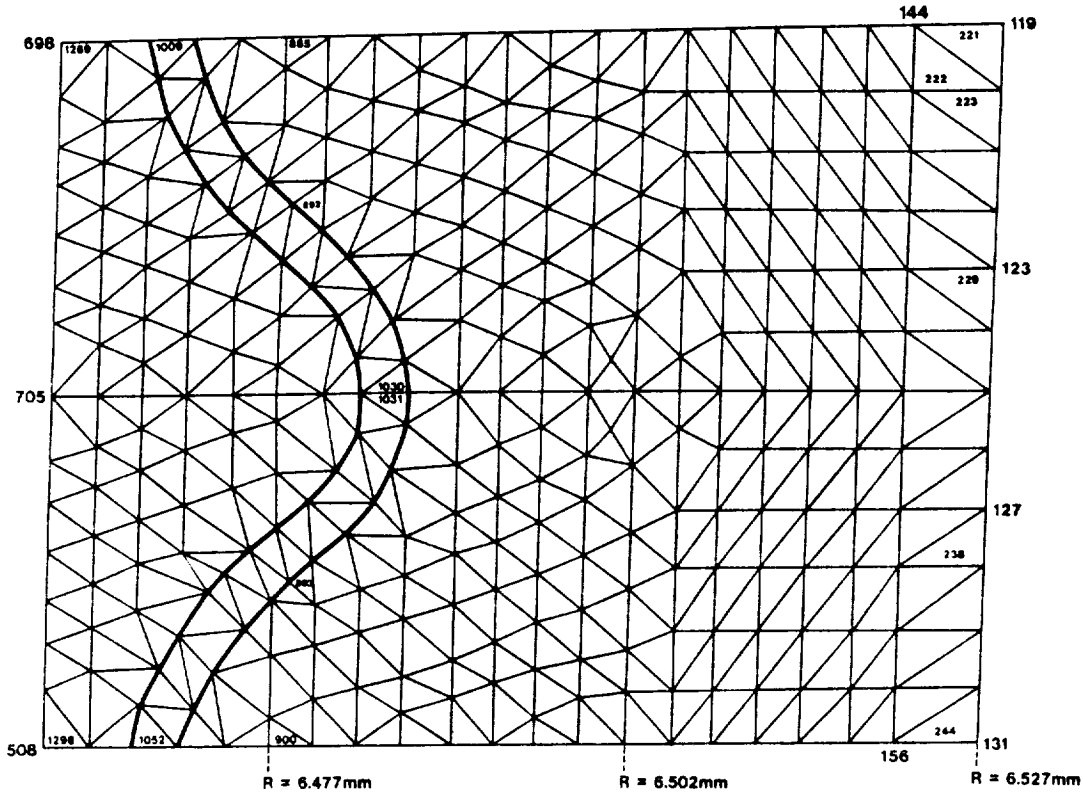

Figure 9. FINITE ELEMENT DETAILS (Part 2C)

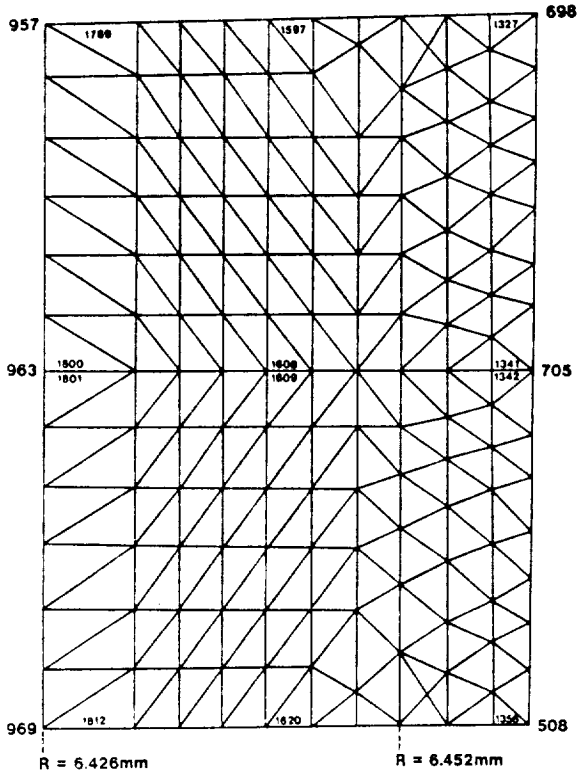

Figure 10. FINITE ELEMENT DETAILS (Part 2D)

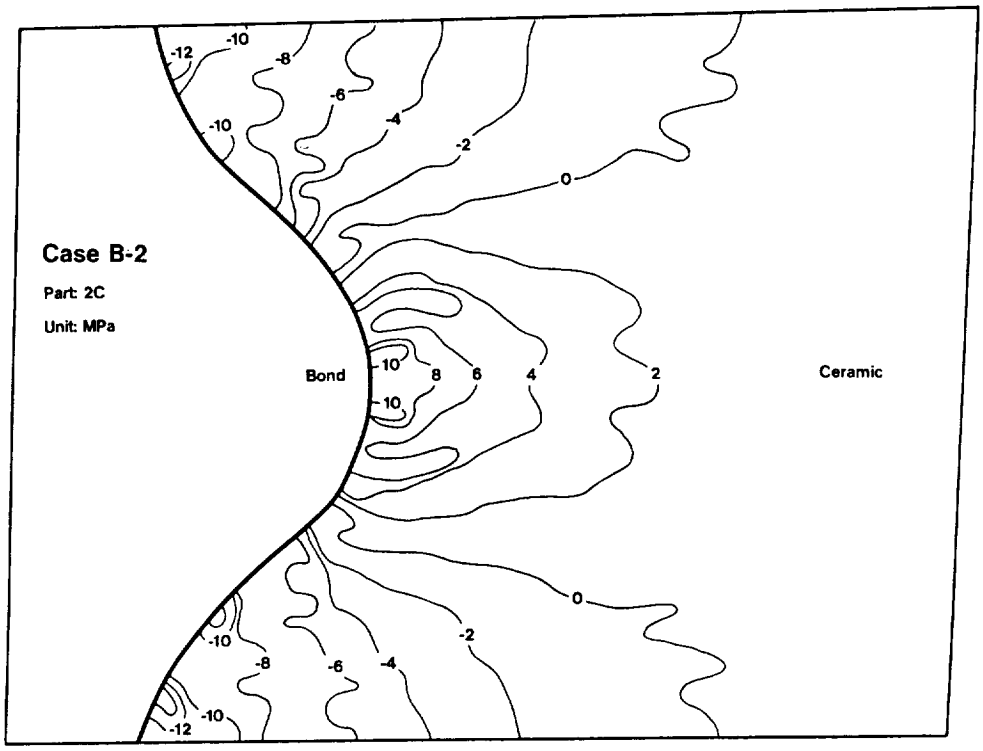

Figure 11. STRESS IN X-DIRECTION DUE TO THERMAL EXPANSION MISMATCH

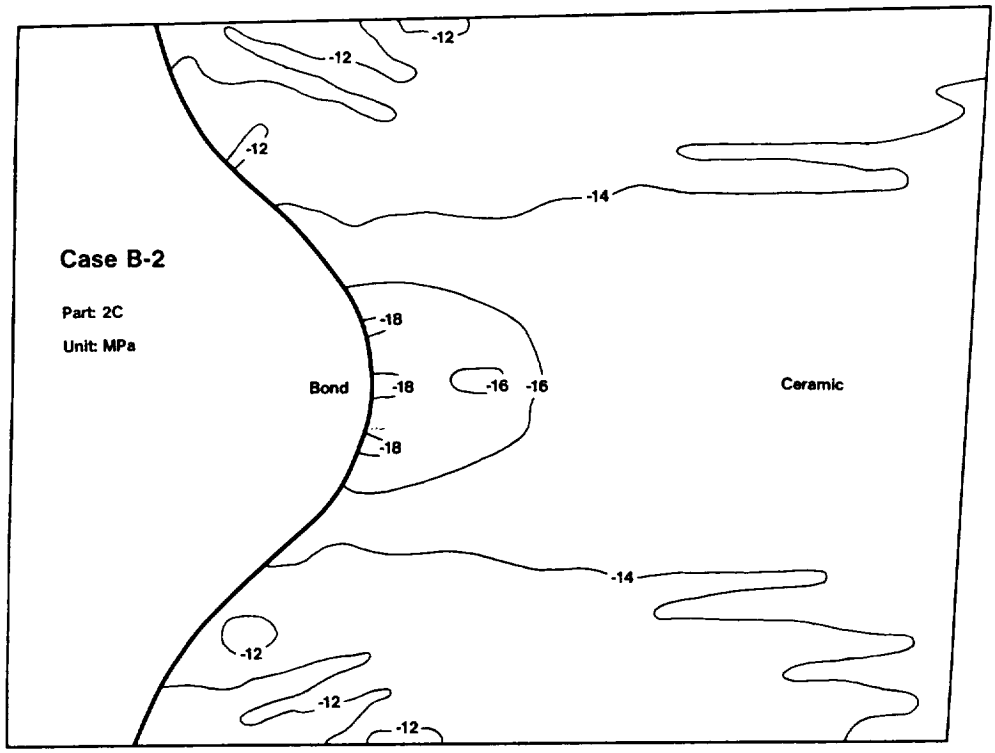

Figure 12. STRESS IN Y-DIRECTION DUE TO THERMAL EXPANSION MISMATCH

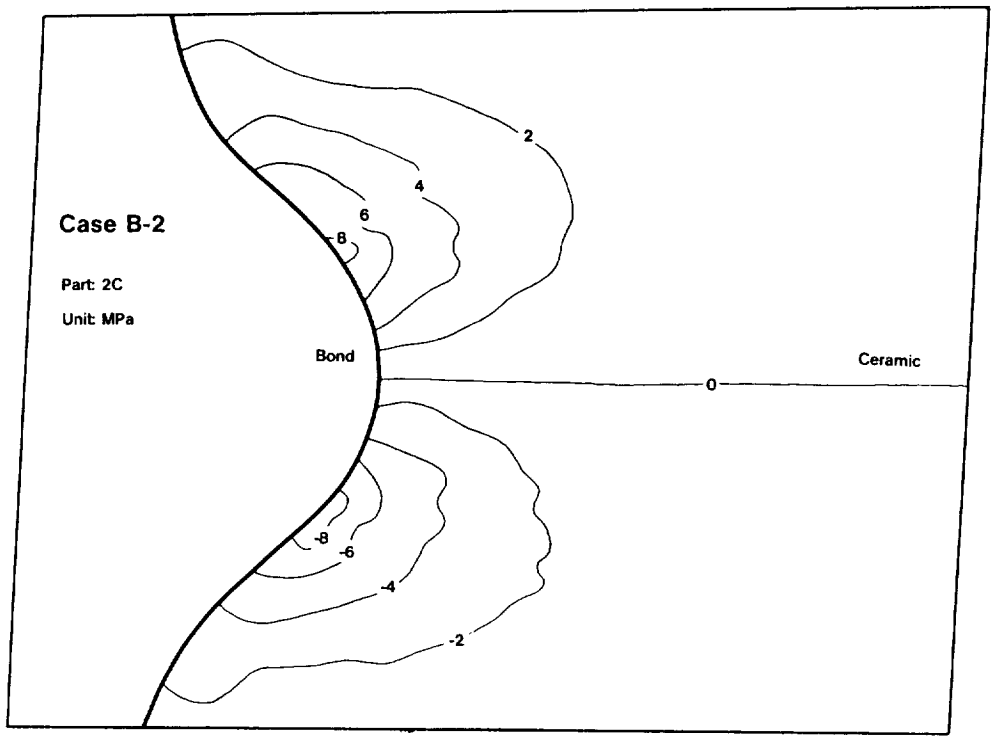

Figure 13. SHEARING STRESS DUE TO THERMAL EXPANSION MISMATCH

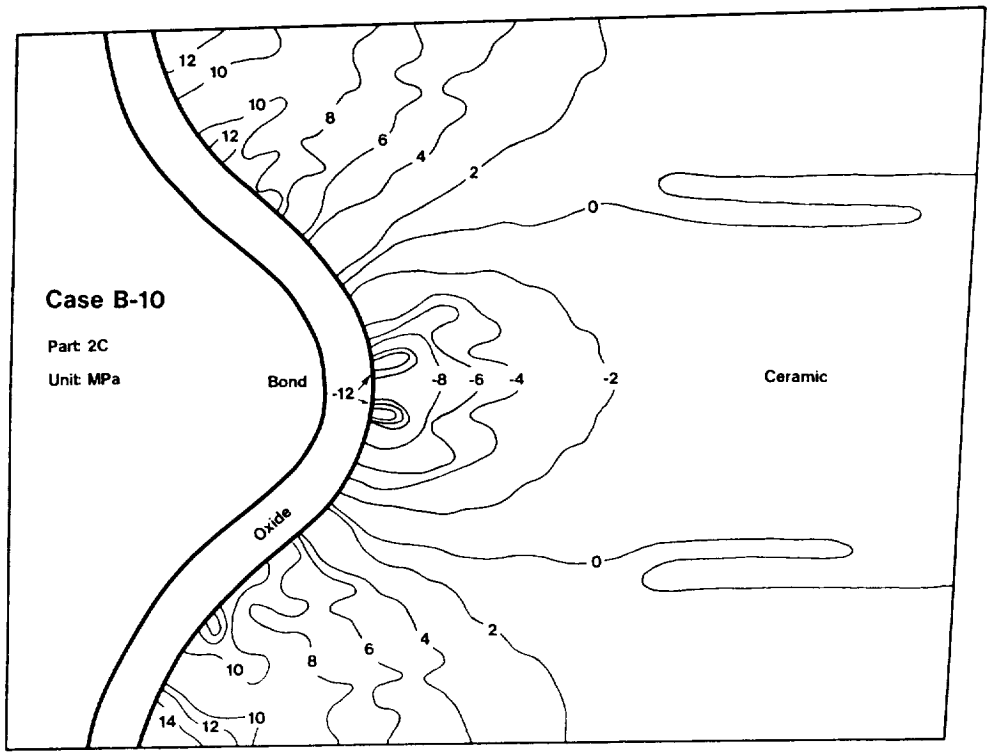

Figure 14. STRESS IN X-DIRECTION DUE TO OXIDATION

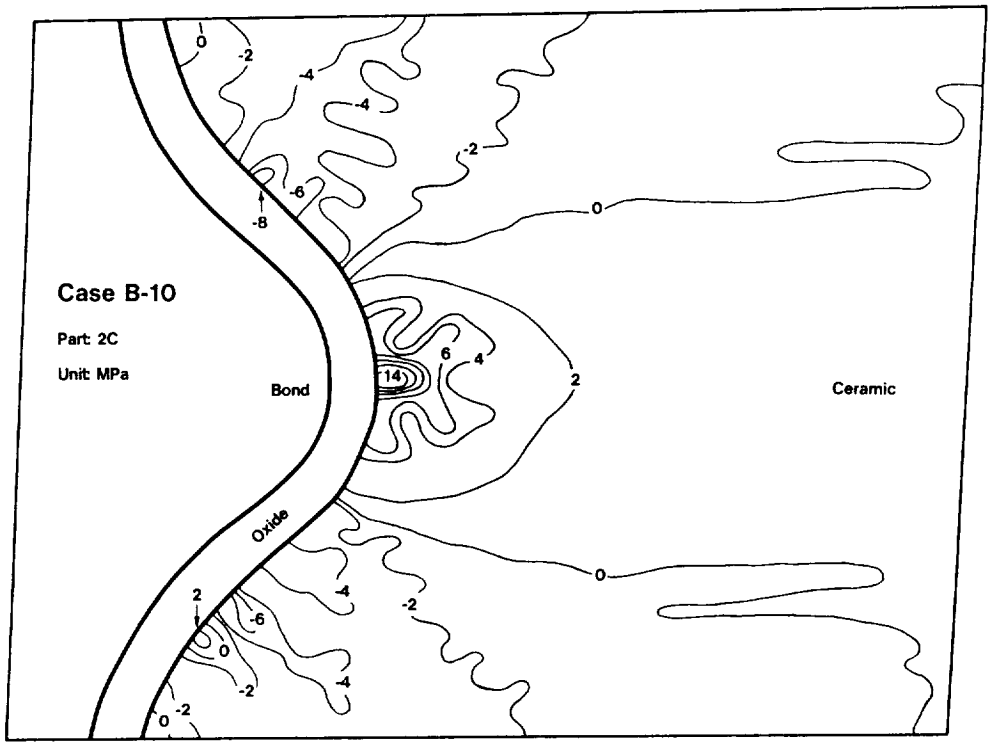

Figure 15. STRESS IN Y-DIRECTION DUE TO OXIDATION

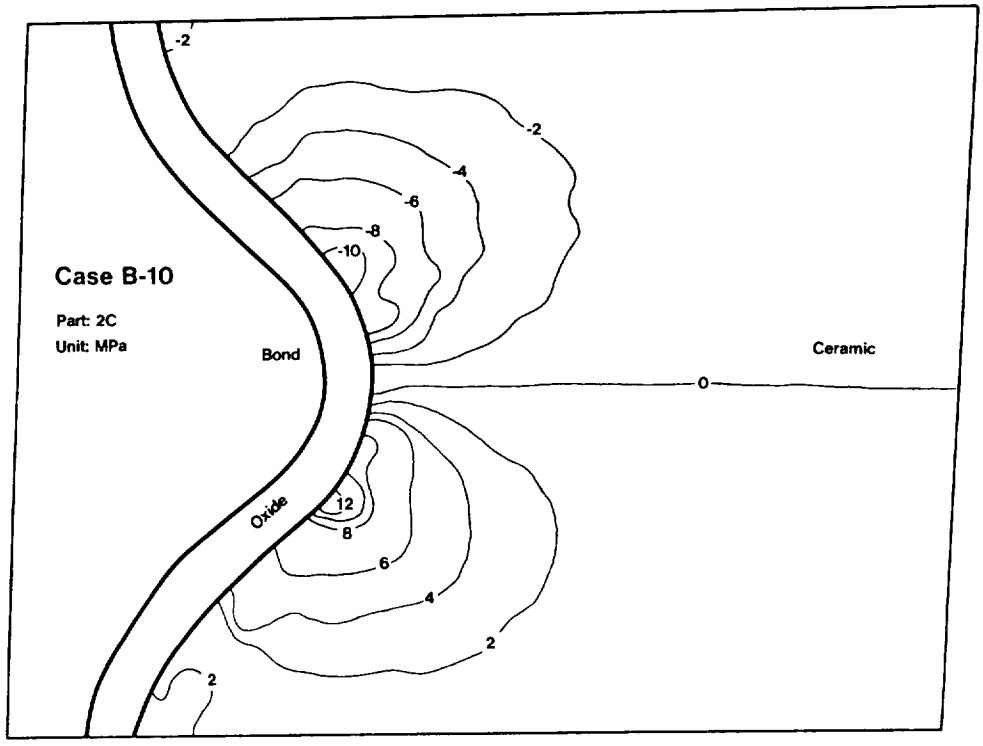

Figure 16. SHEARING STRESS DUE TO OXIDATION

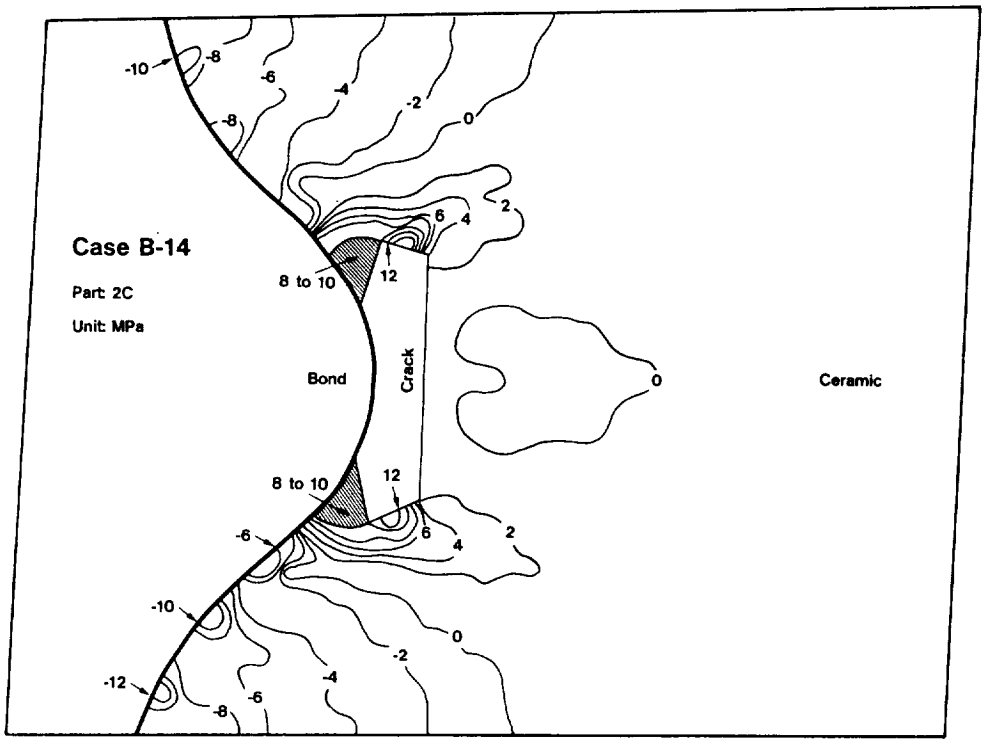

Figure 17. STRESS IN X-DIRECTION DUE TO THERMAL EXPANSION MISMATCH WITH PRECRACKING

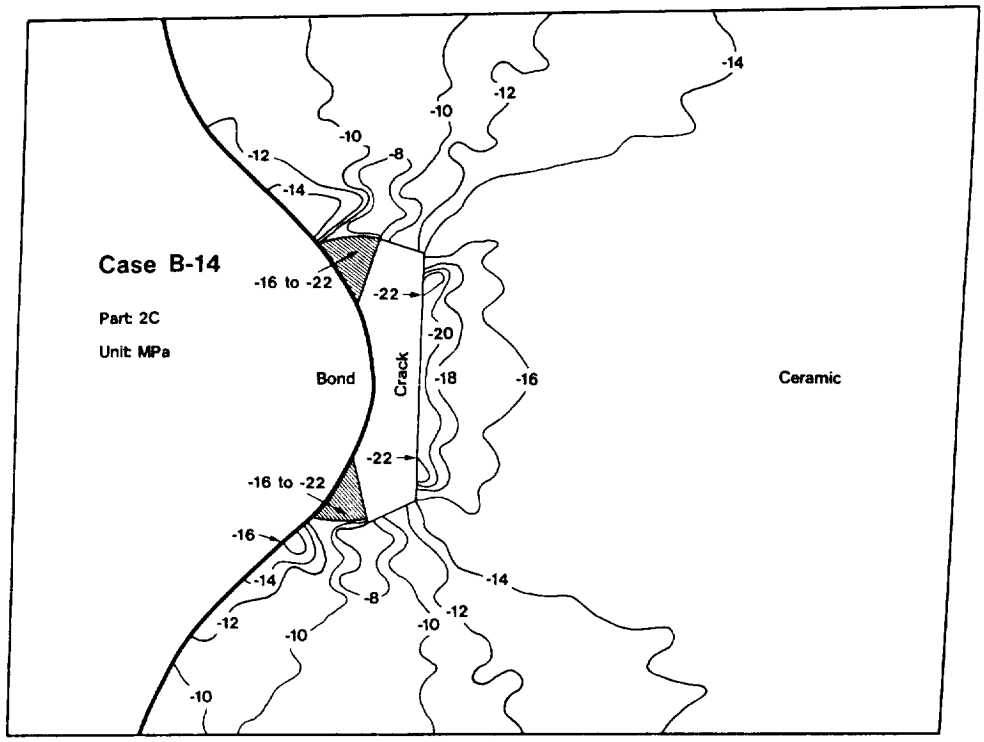

Figure 18. STRESS IN Y-DIRECTION DUE TO THERMAL EXPANSION MISMATCH WITH PRECRACKING

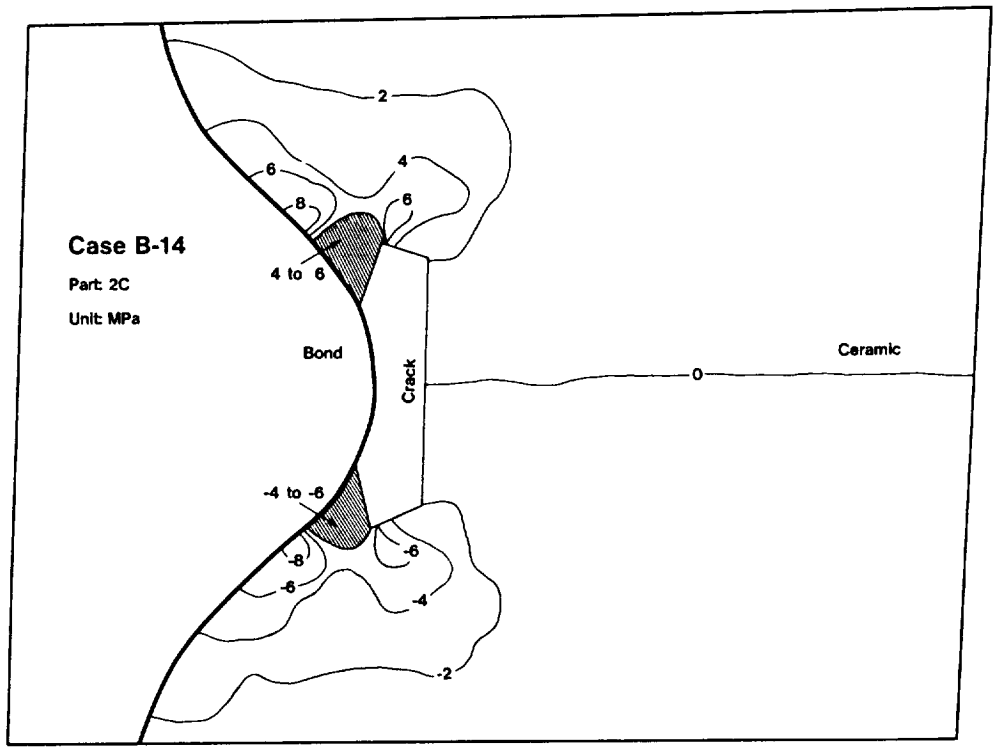

Figure 19. SHEARING STRESS DUE TO THERMAL EXPANSION MISMATCH WITH PRECRACKING

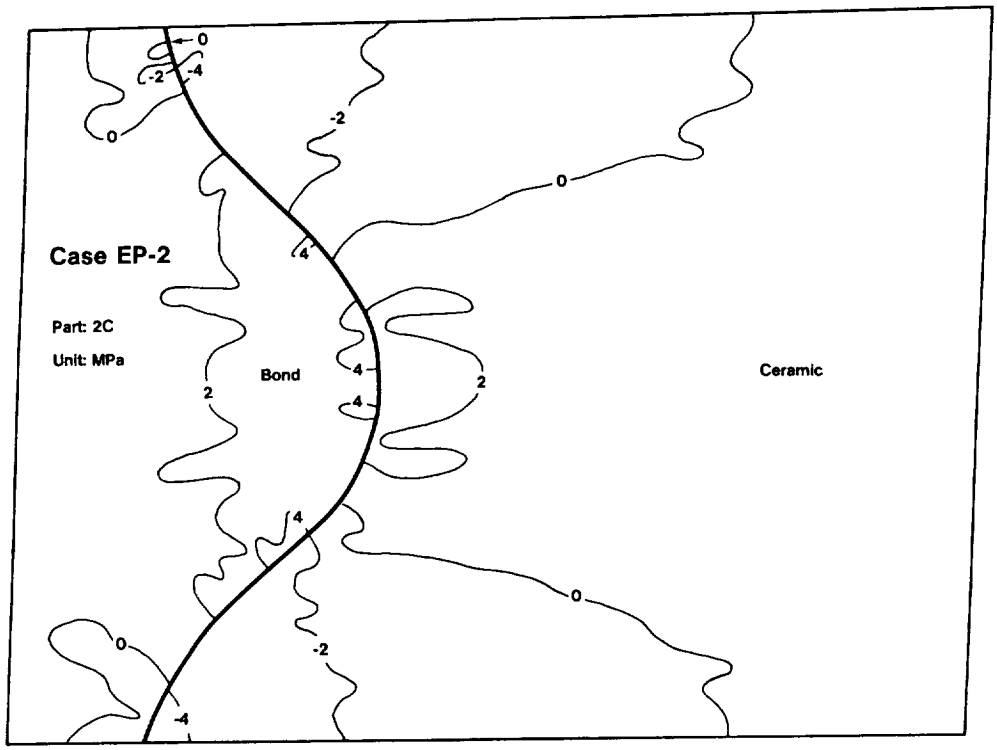

Figure 20. ELASTIC-PLASTIC STRESS IN X-DIRECTION DUE TO THERMAL EXPANSION MISMATCH

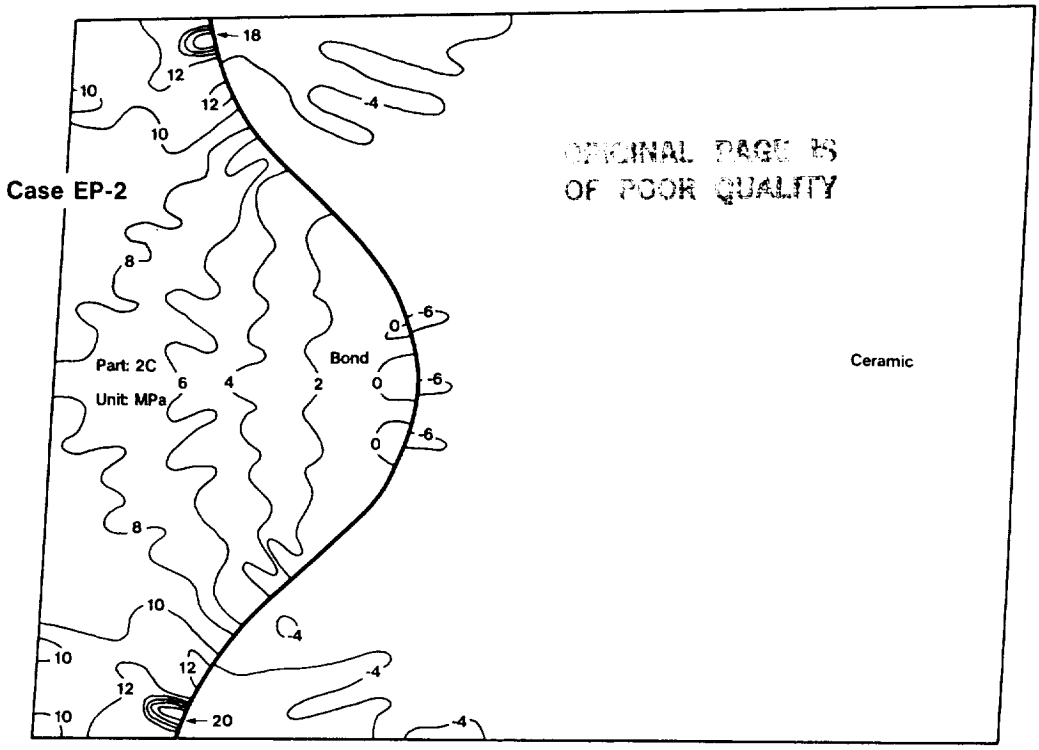

Figure 21. ELASTIC-PLASTIC STRESS IN Y-DIRECTION DUE TO THERMAL EXPANSION MISMATCH

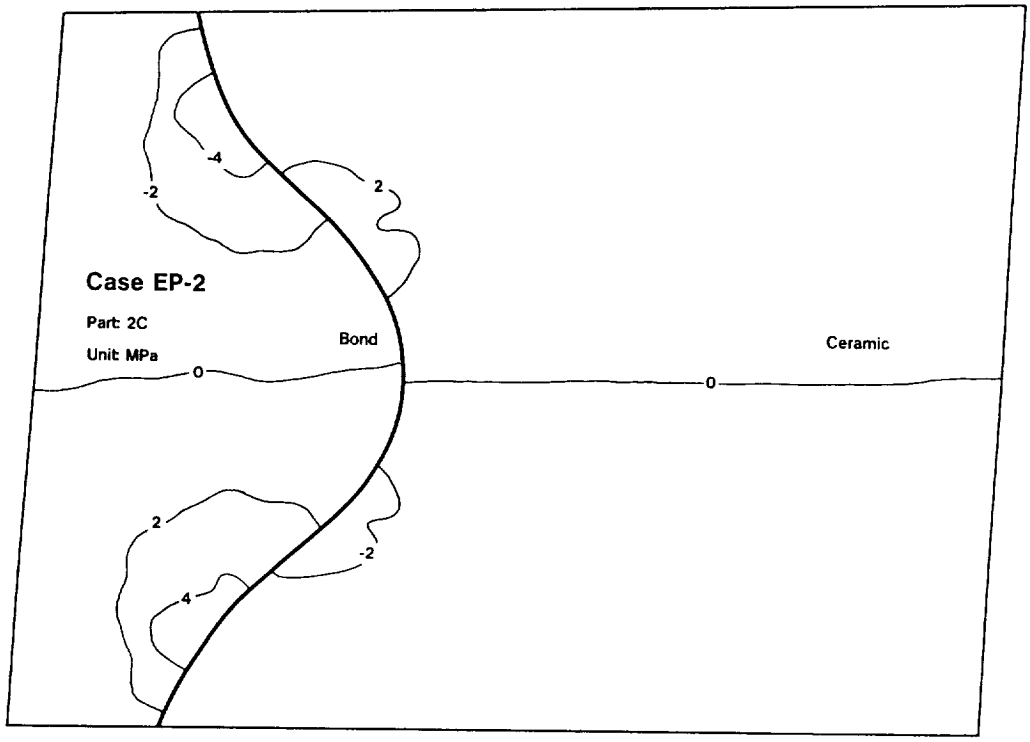

Figure 22. ELASTIC-PLASTIC SHEARING STRESS DUE TO THERMAL EXPANSION MISMATCH